

Alfvén Waves in Bismuth: Charge-Carrier Mass Densities and Relaxation Times

D. S. McLACHLAN

IBM Zurich Research Laboratory, 8803 Rüschlikon-ZH, Switzerland

(Received 6 December 1965; revised manuscript received 18 February 1966)

Alfvén waves in bismuth have been studied in the frequency range 300 to 2000 Mc/sec, for propagation along the magnetic field. All the measurements were done on the same single crystal, and it was found that at the higher frequencies the real part of the dielectric constant is greater than the imaginary and that at lower frequencies the reverse is the case. This frequency dependence had a marked effect on the real part of the refractive index of the medium, which allowed one to measure, in addition to the usual charge-carrier mass density, some mean relaxation time of the charge carriers. The mass densities are in reasonable agreement with theory when the effective masses of the holes and electrons for bismuth from some previous experimental results are used, though there are some inconsistencies, which are discussed. A detailed analysis of the relaxation times proved impractical, but the magnitudes of the values agree well with other experimental results. The effect of Shubnikov-de Haas oscillations on the transmission was also studied.

I. INTRODUCTION

IT has been pointed out by Buchsbaum and Galt¹ that Alfvén waves, first proposed to explain certain phenomena in astrophysics,² could, under certain conditions, propagate in solid-state plasmas. These authors re-interpreted the earlier cyclotron-resonance work of Galt *et al.*³ in terms of Alfvén waves. Since then a number of experiments studying both the reflection and transmission of Alfvén waves have been reported by various workers including Williams,⁴ Williams and Smith,⁵ Kirsch and Miller,⁶ Kirsch,⁷ Khaiken *et al.*,⁸ Khaiken *et al.*,⁹ Bartelink,¹⁰ Kawamura *et al.*,¹¹ and Faughnan.¹² Review articles on Alfvén waves and the closely related subject of helicons have been written by Buchsbaum¹³ and Bowers.¹⁴

With the exception of Bartelink, these workers have been concerned with either the Alfvén-wave velocity (dielectric constant of the medium) or the Doppler-shifted cyclotron resonance of the charge carriers, and so have worked at relatively high frequencies where the damping of the Alfvén waves is small. On the other hand, Bartelink worked at low frequencies where the

waves are heavily damped. The purpose of the present work is to study the propagation of the Alfvén waves in the intermediate-frequency region and to investigate not only the real part of the dielectric constant but also the imaginary part. As all experiments were performed on the same single crystal this allows one to study not only the mass density of the charge carriers but also their relaxation time. The manner in which the Shubnikov-de Haas effect affects the damping of the waves is also studied in some detail.

Section II presents the theory of Alfvén-wave propagation in both anisotropic plasma and an anisotropic plasma. The results for the anisotropic plasma are applied to bismuth and the effects on the propagation of a finite relaxation time, both isotropic and anisotropic, are discussed. In Sec. III the details of the experimental technique are described. The results are presented in Sec. IV and the discussion of these results is in Sec. V.

II. THEORY

i. Alfvén Waves

All the measurements to be discussed in this paper were made where anomalous-skin-effect conditions do not prevail, so that the classical Drude-type theory can be used to discuss the results.

From Maxwell's equations we obtain the wave equation

$$\nabla \times (\nabla \times \mathbf{E}) = (\omega^2/c^2)\epsilon \cdot \mathbf{E}, \quad (1)$$

where the complex dielectric constant is defined as

$$\epsilon = \epsilon_l - i\sigma/\omega\epsilon_0 \text{ (mks units)} \quad (2)$$

with ϵ_l being the lattice dielectric constant and σ the complex conductivity tensor. In the present experiments, ϵ_l which is of the order of 100 can be neglected in comparison with the second term in Eq. (2).

Assuming a plane-wave solution, the wave equation takes the form

$$\mathbf{k} \times (\mathbf{k} \times \mathbf{E}) + k_0^2 \epsilon \cdot \mathbf{E} = 0, \quad (3)$$

¹ S. J. Buchsbaum and J. K. Galt, *Phys. Fluids* **4**, 1514 (1961).

² H. Alfvén, *Cosmical Electrodynamics* (Clarendon Press, Oxford, 1950).

³ J. K. Galt, W. A. Yager, F. R. Merrit, B. B. Celnit, and A. D. Brailsford, *Phys. Rev.* **114**, 1396 (1959).

⁴ G. A. Williams, *Phys. Rev.* **139**, A771 (1965).

⁵ G. A. Williams and G. E. Smith, *IBM J. Res. Develop.* **8**, 276 (1964).

⁶ J. Kirsch and P. B. Miller, *Phys. Rev. Letters* **9**, 421 (1962).

⁷ J. Kirsch, *Phys. Rev.* **133**, A1390 (1964).

⁸ M. S. Khaikin, V. S. Edel'man, and R. T. Mina, *Zh. Eksperim. i Teor. Fiz.* **44**, 2190 (1963) [English transl.: *Soviet Phys.—JETP* **17**, 1470 (1963)].

⁹ M. S. Khaikin, La Fal'kovskii, V. S. Edel'man, and R. T. Mina, *Zh. Eksperim. i Teor. Fiz.* **45**, 1704 (1963) [English transl.: *Soviet Phys.—JETP* **18**, 1167 (1964)].

¹⁰ D. J. Bartelink, *Bull. Am. Phys. Soc.* **8**, 205 (1963).

¹¹ H. Kawamura, S. Nagata, T. Nakama, and S. Takano, *Phys. Letters* **15**, 111 (1965).

¹² B. W. Faughnan, *J. Phys. Soc. Japan* **20**, 574 (1965).

¹³ S. J. Buchsbaum, *Symposium on Plasma Effects in Solids* (Dunod Cie., Paris, 1964).

¹⁴ R. Bowers, *Symposium on Plasma Effects in Solids* (Dunod Cie., Paris, 1964).

where $k_0^2 = \omega^2/c^2$. If the direction of the steady magnetic field \mathbf{B} and the direction of propagation are both chosen along the z axis ($\mathbf{k} \parallel \mathbf{B}$), the dispersion equation is

$$\begin{vmatrix} k_0^2 \epsilon_{xx} - k^2 & k_0^2 \epsilon_{xy} & 0 \\ -k_0^2 \epsilon_{xy} & k_0^2 \epsilon_{yy} - k^2 & 0 \\ 0 & 0 & k_0^2 \epsilon_{zz} \end{vmatrix} = 0. \quad (4)$$

This can be solved using Eq. (2) and neglecting ϵ_i to give

$$\epsilon = k^2/k_0^2 = (1/i\omega\epsilon_0)^{1/2} (\sigma_{xx} + \sigma_{yy}) \pm \left[\frac{1}{2} (\sigma_{xx} - \sigma_{yy})^2 - \sigma_{xy}^2 \right]^{1/2}. \quad (5)$$

This equation defines the dielectric constant due to the charge carriers. It is also possible to obtain a solution when \mathbf{k} is not parallel to \mathbf{B} but the above equation covers the only case considered in this work.

In the classical skin-effect limit, the complex conductivity can be obtained by solving the equation of motion for the charge carriers.

$$\mathbf{m} \cdot \frac{d\mathbf{v}}{dt} + \frac{q\mathbf{B}}{m_0} \times \mathbf{v} + \nu \mathbf{m} \cdot \mathbf{v} = \frac{q\mathbf{E}}{m_0}, \quad (6)$$

where \mathbf{m} is the effective mass of the charge carriers in terms of the free electron mass m_0 , \mathbf{v} is the drift velocity of the charge carrier, \mathbf{B} the large static magnetic field and $\nu \equiv 1/\tau$ is the collision frequency and τ the relaxation time of the charge carriers (both of which are assumed to be isotropic).

This equation has been put in the form

$$\sigma/\sigma_0 = (\mathbf{m} + \mathbf{b} \times \mathbf{1})^{-1}, \quad (7)$$

where $\mathbf{1}$ is the identity matrix,

$$\begin{aligned} \mathbf{b} &= q\mathbf{B}/(\nu + i\omega)m_0, \\ \sigma_0 &= nq^2/(\nu + i\omega)m_0, \end{aligned}$$

and solved by Lax *et al.*¹⁵ However, these results are cumbersome and a better understanding of the physics involved is obtained from the equations for an isotropic plasma. The formulas for an isotropic plasma will not of course apply to bismuth, and more complicated formulas will have to be developed later.

ii. Isotropic Plasma

For an isotropic plasma of electrons and holes the dielectric constant can be written, in the limits $\omega_{ce}\tau \gg 1$ and $\omega_{ch}\tau \gg 1$ and ω_{ce} and $\omega_{ch} \gg \omega$, as

$$\begin{aligned} \epsilon_{xx} = \epsilon_{yy} &= \left[\frac{\omega_{pe}^2}{\omega_{ce}^2} + \frac{\omega_{ph}^2}{\omega_{ch}^2} \right] \left(1 - \frac{i}{\omega\tau} \right), \\ &= \frac{(n_e m_e + n_h m_h)}{\epsilon_0 B^2} \left(1 - \frac{i}{\omega\tau} \right), \\ &= \frac{\mu_0 (n_e m_e + n_h m_h)}{B^2} c^2 \left(1 - \frac{i}{\omega\tau} \right), \end{aligned} \quad (8)$$

¹⁵ B. Lax, K. J. Button, H. J. Zeiger, and L. Roth, Phys. Rev. **102**, 715 (1956).

$$\begin{aligned} \epsilon_{xy} &= -\epsilon_{yx} = i \left[-(\omega_{pe}^2/\omega\omega_{ce}) + (\omega_{ph}^2/\omega\omega_{ch}) \right], \\ &= i(q/\epsilon_0 B\omega) (-n_e + n_h), \end{aligned} \quad (9)$$

$$\epsilon_{zz} = 1 - \omega_{pe}^2/\omega^2 - \omega_{ph}^2/\omega^2, \quad (10)$$

where

$$\begin{aligned} \omega_{ce} &= (qB/m_e) \text{ (electron cyclotron frequency),} \\ \omega_{ch} &= (qB/m_h) \text{ (hole cyclotron frequency),} \\ \omega_{pe}^2 &= (n_e q^2/\epsilon_0 m_e) \text{ (electron plasma frequency)}^2, \\ \omega_{ph}^2 &= (n_h q^2/\epsilon_0 m_h) \text{ (hole plasma frequency)}^2. \end{aligned}$$

When $|\epsilon_{xy}| \gg \epsilon_{xx}$, one gets as a propagating wave a circularly polarized helicon. In a compensated material such as bismuth $n_e \approx n_h$ and $\epsilon_{xx} \gg |\epsilon_{xy}|$, so that the propagating wave is a linearly polarized Alfvén wave.

The experimentally measured quantity is the refractive index μ , the real and imaginary parts of which are

$$\mu_r = \left[\frac{\mu_0 (n_e m_e + n_h m_h) c^2}{B^2} \right]^{1/2} \left\{ \frac{1 + [1 + (1/\omega\tau)^2]^{1/2}}{2} \right\}^{1/2}, \quad (11)$$

$$\begin{aligned} \mu_i &= -\frac{i}{2\omega\tau} \left[\frac{\mu_0 (n_e m_e + n_h m_h) c^2}{B^2} \right]^{1/2} \\ &\quad \left\{ \frac{1 + [1 + (1/\omega\tau)^2]^{1/2}}{2} \right\}^{-1/2}. \end{aligned} \quad (12)$$

If the real part of the refractive index is measured at two angular frequencies, preferably with one greater than and the other somewhat less than $1/\tau$, one can obtain both the mass density $(n_e m_e + n_h m_h)$ and the relaxation time.

These formulas now have to be extended to cover the case of bismuth, which is anisotropic. Before this is done, a brief description of the Fermi surface of bismuth is necessary.

iii. Fermi Surface of Bismuth

The model of the band structure most frequently used to discuss experiments is the tilted ellipsoidal model, which has recently been reviewed by Boyle and Smith.¹⁶ In this model the electrons are described as being located in k space by three ellipsoids¹⁷ slightly rotated about the binary axis out of the plane perpendicular to the trigonal axis. The energy of an electron within an ellipsoid is given by

$$E = (\hbar^2/2m_0) (\alpha_1 k_1^2 + \alpha_2 k_2^2 + \alpha_3 k_3^2 + 2\alpha_4 k_2 k_3), \quad (13)$$

where k_1 , k_2 , and k_3 are the wave-vector components parallel to the binary, bisectrix, and trigonal axis, respectively, and the α 's are components of the re-

¹⁶ W. S. Boyle and G. E. Smith, in *Progress in Semiconductors*, edited by A. F. Gibson (Heywood and Company, Ltd., London, 1960), Vol. 7.

¹⁷ A. L. Jain and S. H. Koenig, Phys. Rev. **127**, 442 (1962).

reciprocal mass tensor. [The bisectrix axis (2) is at right angles to both the trigonal axis (3) and one of the three binary axes (1).] The effective mass tensor for an electron in such an ellipsoid is

$$\begin{pmatrix} m_1 & 0 & 0 \\ 0 & m_2 & m_4 \\ 0 & m_4 & m_3 \end{pmatrix}, \quad (14)$$

where m_1 , m_2 , m_3 , and m_4 are in units of the free-electron mass. The two remaining ellipsoids are obtained by 120° rotations about the trigonal axis.

The hole band is much simpler, consisting of a single ellipsoid of revolution about the trigonal axis, the energy of a hole being given by

$$E = \left(\frac{\hbar^2}{2m_0} \right) \left(\frac{k_1^2}{M_1} + \frac{k_2^2}{M_1} + \frac{k_3^2}{M_3} \right),$$

where M_1 and M_3 are the effective masses of the holes, again in terms of the free electron mass.

iv. Anisotropic Theory

The magneto-conductivity using the model discussed above has been calculated by Lax *et al.*¹⁵ from Eq. (7), with an isotropic relaxation time. The conductivities to be substituted in Eq. (5) are the high-field limits of the results of Lax *et al.* [In the anisotropic case even where $n_e = n_h$ the dielectric tensor is not diagonal, but with B along the principal axis, $nf(m)$ is unaffected by the off-diagonal terms in the high-field limit.] The expression for the velocity of the Alfvén wave (v_A) can now be written as

$$v_A^2 = B^2 / \mu_0 m_0 n f(m) F, \quad (15)$$

where

$$F = \frac{1}{2} [1 + (1 + (1/\omega\tau)^2)^{1/2}] \quad (16)$$

and $nf(m)$ is the mass density of the medium, where n is the number of charge carriers per cubic meter and $f(m)$ is a function of the effective masses of the holes and electrons obtained from the results of Lax *et al.*

It can be seen from Eqs. (4) and (5) that the dielectric constant and hence the function $nf(m)$ depends not only on the direction of the magnetic field but also on the direction of the electric field of the incident wave. The expressions for $nf(m)$ for all the configurations used in these experiments are shown in Table I.

However, because of the anisotropy of bismuth it is obvious that the relaxation time of bismuth is not isotropic, so that the procedure outlined above is only determining some mean relaxation time or, to be more precise, the ratio of the real to the imaginary part of the dielectric constant.

The procedure due to Lax *et al.* can be generalized to take into account an anisotropic relaxation time or an anisotropic mobility tensor (which is not just a constant multiple of the mass tensor). This procedure is general-

ized by assuming a mobility tensor of the form

$$\begin{pmatrix} \beta_1 & 0 & 0 \\ 0 & \beta_2 & \beta_4 \\ 0 & \beta_4 & \beta_3 \end{pmatrix} \quad (17)$$

which has an inverse of the form

$$\begin{pmatrix} \gamma_1 & 0 & 0 \\ 0 & \gamma_2 & \gamma_4 \\ 0 & \gamma_4 & \gamma_3 \end{pmatrix}. \quad (18)$$

The equation of motion of an electron in a large static magnetic field, an alternating electric field ($\mathbf{E} = \mathbf{E}_0 e^{i\omega t}$) and for an isotropic relaxation time τ is given by

$$\mathbf{m}' \cdot (d\mathbf{v}/dt) + q\mathbf{B} \times \mathbf{v} + (\mathbf{m}'/\tau) \cdot \mathbf{v} = q\mathbf{E} \quad (19)$$

which can be generalized to

$$(i\omega/q)\mathbf{m}' \cdot \mathbf{v} + \mathbf{B} \times \mathbf{v} + \boldsymbol{\gamma} \cdot \mathbf{v} = \mathbf{E} \quad (20)$$

from which

$$\mathbf{v} = [(i\omega\mathbf{m}'/q + \boldsymbol{\gamma} + \mathbf{B} \times \mathbf{I})^{-1} \cdot \mathbf{E}. \quad (21)$$

\mathbf{m}' in the above equations is $m\mathbf{m}_0$. There is now a one as to one correspondence with Eq. (22) of Lax *et al.* and, using the fact that $\mathbf{J} = nev$, with Eq. (7) in this paper. This correspondence can be used to calculate the high-field limits of the conductivity tensor and hence the dielectric tensor.

The correspondence of Eq. (22) of Lax *et al.* and Eq. (7) with the above Eq. (21) is

$$\begin{aligned} \mathbf{m} &= (i\omega\mathbf{m}'/q + \boldsymbol{\gamma}), \\ \mathbf{b} &= \mathbf{B}, \\ \sigma_0 &= nq, \end{aligned}$$

and the high-field limit corresponds to

$$|B| \gg |i\omega\mathbf{m}'/q + \boldsymbol{\gamma}|.$$

From the above, one obtains for the dielectric-tensor components

$$\begin{aligned} \epsilon &= -i\sigma/\omega\epsilon_0. \\ &= -i \frac{nq f[i\omega\mathbf{m}'/q + \boldsymbol{\gamma}]}{\epsilon_0 B^2}, \end{aligned}$$

where the $f(i\omega\mathbf{m}'/q + \boldsymbol{\gamma})$ for each orientation of the electric and magnetic field is obtained from Table I replacing the m_i (and M_i) in these formulas by

$$i\omega m'_i / q + \gamma_i.$$

It is seen that since the equations for $f(i\omega\mathbf{m}'/q + \boldsymbol{\gamma})$ are not linear one obtains cross terms, and cannot separate a real part of the dielectric constant involving only terms in $\omega m'_i / q$ from the imaginary part involving only terms in γ_i . This, naturally, greatly complicates the analysis of the results.

It should be remarked here that so far, quantum effects have not been taken into account. These arise because in the presence of a magnetic field the electrons

TABLE I. Expressions for $nf(m)$, the values of $[nf(m)]^{1/2}$ and τ measured. The values of τ in brackets indicate the maximum possible uncertainty in τ for these experiments. [Note that $M_1=M_2$ due to the symmetry of bismuth.]

$H $ axis	$E $ axis	Dielectric constant	$nf(m)$	$[nf(m)]^{1/2} \times 10^{-9}$	Relaxation time τ (nsec)
1	2	ϵ_{22}^1	$n\{m_3 - 2m_4^2/(m_1 + 3m_2) + M_3\}$	0.429	0.21(0.24-0.18)
1	3	ϵ_{33}^1	$n\{\frac{1}{3}m_2 + (8/3)m_1m_2/(m_1 + 3m_2) + M_3\}$	0.363	0.55(1.0-0.35)
2	1	ϵ_{11}^2	$n\{m_3 - m_4^2/3m_2 - \frac{2}{3}m_4^2/(3m_1 + m_2) + M_3\}$	0.461	0.37(0.50-0.28)
2	3	ϵ_{33}^2	$n\{\frac{1}{3}m_1 + (8/3)m_1m_2/(3m_1 + m_2) + M_1\}$	0.146	0.15(0.17-0.12)
3	1	ϵ_{11}^3	$\frac{1}{2}n\{(m_1 + m_2) - m_4^2/m_3 + 2M_3\}$	0.315	0.27(0.34-0.23)
3	2	ϵ_{22}^3	$\frac{1}{2}n\{(m_1 + m_2) - m_4^2/m_3 + 2M_1\}$	0.304	0.22(0.27-0.18)

quantize into the well-known Landau levels which, due to a changing magnetic field, pass through the Fermi surface giving rise to oscillations both in the relaxation time of the charge carriers and the mass density itself. The effect of the changing mass density is small, and as will be seen later, does not greatly influence the results. The effect of the changing relaxation time (Shubnikov-de Haas effect) also clearly shows up in the experimental results. The fact that the relaxation time is an oscillating function of the magnetic field means that the relaxation time measured is an average over the magnetic field range in which the experiment is done.

III. EXPERIMENTAL DETAILS

All the measurements described here were made on a single sample of bismuth, which was a cube, oriented along the principal axes, with a 7-mm edge. The sample was spark-cut from a single crystal, which had been grown from bismuth of quoted purity better than 0.999999 (purchased from Cominco Company) using a traveling-zone technique. The surfaces of the cube were spark planed and the damaged layer removed chemically. The alignment along the trigonal axis was to better than 1° , along the other axes to better than 2° . A residual resistivity ratio $\rho_{293}/\rho_{4.2}$ of 120 was measured, with the current along the trigonal axis, in a sample cut from the same single crystal adjacent to the above mentioned cube.

A block diagram of the apparatus used is shown in Fig. 1 and a schematic diagram of the sample holder is

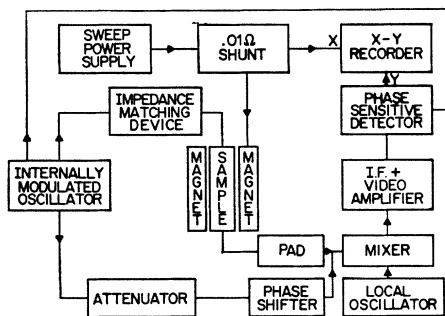


FIG. 1. Block diagram of apparatus used in the experiments.

shown in Fig. 2. A signal (300–2000 Mc/sec), which was modulated at 1000 cps, was fed from the oscillator through an impedance matching device (trombone line and stub) into a strip line and then through a short length of waveguide beyond cutoff (in the TE_{01} mode) to the surface of the sample where it excited an Alfvén wave. The strip line and waveguide ensured an electric field of known orientation. As the sample was larger than the waveguide ($5 \times 2\frac{1}{2}$ mm) it completely covered the end of it. In order to cut down the leakage signal, the sample was glued against the sidewalls of the waveguide with silver paste and an iris was glued with silver paste between the sample and the pickup coil. The signal (Alfvén wave) transmitted through the sample was detected by this pickup loop and fed through a 10-dB matching pad into a mixer, i.f., and video amplifier before going into a phase-sensitive detector. It was also possible to couple a reference signal (used to measure the relative phase of the transmitted signal) into the mixer via an attenuator and phase shifter. The output of the phase sensitive detector drove the y axis of an x-y recorder, the x axis of which measured the current in the 40-kG superconducting coil used in these experiments.

For a given frequency, as the magnetic field and hence the number of wavelengths in the sample changes, it is possible, if the attenuation is low enough, to get Fabry-Perot or standing-wave resonances. However, in these experiments, this effect was only observable with low frequencies at the highest magnetic fields used, so that a reference signal had to be added in order to obtain interference or phase oscillations corresponding to a change of one wavelength in the sample.

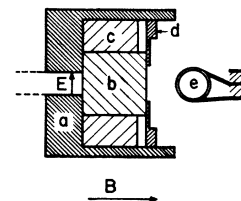


FIG. 2. Schematic cross-sectional diagram of sample holder. a is the waveguide beyond cutoff excited from the left by a strip line. b is the sample. c is a sprung Plexiglass sample holder. d is the iris. e is the pickup loop. The small arrow indicates the direction of the electric field (E), the large that of the magnetic field (B).

When no reference signal was added, it was possible to observe the transmission envelope at higher fields. Interference oscillations with the unavoidable leakage signal were observed when the magnetic field and hence the transmitted signal were too low.

When a reference signal is added, maxima occur when

$$(N + \delta) = d\mu f/c,$$

where N is the fringe index, d the sample thickness, f the frequency of the electromagnetic wave, and δ is an arbitrary phase factor depending on the relative phase of the reference signal. Propagation is normal to the surface so there is no $\cos\theta$ term.

The simple theory for an infinite medium is used here with no account being taken of the fact that the sample is finite in the directions perpendicular to the magnetic field. This can be justified by noting that the sample has a very high refractive index, typically 100 or more, which ensures that the wave propagation is always normal to the surface except for diffraction effects. However, when diffraction effects are calculated it is found that even for the shortest wavelengths observed in the medium, the central maximum of the diffraction pattern completely covers the opening of the iris. It should also be noted that any wave striking the surface at all obliquely will undergo total internal reflection, and because of the high attenuation in the medium, play no further role.

The refractive index μ for an anisotropic medium as a function of magnetic field, can be found from Eq. (15). From this it can be seen that if one plots N versus $1/B$, the slope of the resulting straight line gives $[nf(m)F]^{1/2}$. Therefore by measuring the slope of the line for two different frequencies both $nf(m)$ and τ can be deduced (in the isotropic τ approximation).

However, as previously shown, an analysis of bismuth for an anisotropic relaxation time involves cross terms, and hence this simple procedure for the separation of the real and imaginary parts is not valid. Calculation of $f(m)$ using the effective masses of Smith, Baraff, and Rowell¹⁸ (hereafter referred to as SBR) shows, however, that for ϵ_{22}^1 , ϵ_{33}^1 , and ϵ_{11}^2 (the superscript refers to the direction of the magnetic field) the contribution to $f(m)$ from the nonlinear terms is 1% or less. Therefore for these orientations, the effect of the nonlinear terms should be negligible, so that the procedure of separating real and imaginary parts outlined earlier should be valid. For ϵ_{33}^2 the cross term contributes 17% of $f(m)$ so the procedure is less accurate. For ϵ_{11}^3 and ϵ_{22}^3 , where the nonlinear term is the negative one and has a magnitude of 30% of the sum of the positive terms, the procedure is questionable.

Data were taken at both 4.2°K and 1.5°K. All measurements of relaxation times and mass densities shown in Table I was taken at 4.2°K. The data taken

at 1.5°K were principally to show the effect of the quantum oscillations (Shubnikov-de Haas and mass density) more clearly.

IV. RESULTS

Figure 3 shows a set of interference fringes at 1.5°K with the magnetic field parallel to the bisectrix axis and the electric field parallel to the binary axis at a frequency of 1.705 kmc/sec. These results clearly show the type of curves obtained. The lower temperature enhances the modulation due to the Shubnikov-de Haas effect.

Figure 4 shows that when the fringe indices of the maxima and minima are plotted against $1/B$ one does not obtain a straight line but that the experimental points oscillate slightly. This is due to the mass density changing with the magnetic field. The line drawn through the points is a least-squares line, the slope of which is used to determine the mass density.

The oscillations obtained here are in qualitative agreement with those obtained by Williams and Smith.⁵ As these authors have already dealt with the matter in some detail it will not be further discussed here. The value obtained for the mass density does however depend very slightly upon the range in which the data is taken, providing, of course, the range is sufficiently large.

The accuracy with which the refractive indices are measured depends upon the frequency range. At the higher frequencies (1500–2000 Mc/sec) there is a relatively large number of maxima and minima and therefore a very small (less than 1%) standard deviation when these points are fitted to a straight line (N versus $1/B$) using a rms procedure. It is also observed that the refractive indices obtained for different phases of the reference signal differ by at most 1%. As other sources of error do not total more than 1%, the total error at these higher frequencies is less than 2%.

At the lower frequencies (300–500 Mc/sec) there are fewer maxima and minima and hence the resulting straight lines have a larger standard error. To improve the accuracy of the results, data is taken for a large

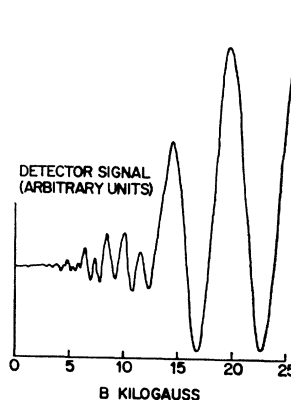


FIG. 3. Interference fringes in the bismuth sample at 1.5°K. The magnetic field was parallel to a bisectrix axis and the electric field was parallel to a binary axis. The frequency was 1.705 Gc/sec.

¹⁸ G. E. Smith, G. A. Baraff, and J. M. Rowell, Phys. Rev. 135, A1118 (1964).

number of different reference phases. The refractive indices obtained for the same frequency and different reference phases deviate from the mean by no more than 3%. When a 1% error due to other sources is included, the results for the refractive indices at the lower frequencies have a maximum error of 4%.

At lower frequencies and higher fields, when the wavelength in the sample is $2d$ ($d \approx 7$ mm) or occasionally d , some effects due to standing-wave resonances become apparent. This sometimes has the effect of causing a double peak or of moving an interference maximum or minimum slightly from where it should lie. After the point where $d = \frac{1}{2}\lambda$, the signal decreases strongly giving the appearance of a waveguide-type cutoff, but this is only due to the approaching $\frac{1}{4}\lambda$ minima. (This was checked using a sample $10 \times 7 \times 7$ mm.) These effects cause no confusion as they can easily be identified by changing the phase of the reference signal. The fact that there are no wave-guide effects¹⁸ for this geometry clearly indicates that using the infinite-medium theory to analyze the results is quite justified.

As the frequency correction to the mass densities obtained at the higher frequencies is less than 2% except for ϵ_{33}^2 , the error in $[nf(m)]^{1/2}$ for orientations where the cross terms are small should be no more than 2%. In the other orientations, faulty separation of the real and imaginary parts makes error estimation difficult but nowhere is it likely to exceed 5%. The results for all six orientations are shown in Table I. The values of $[nf(m)]^{1/2}$ and τ are obtained by the procedure outlined earlier, assuming that Eq. (15) is valid in all cases. All six orientations shown in this table were measured first and then four of these were repeated. The values of $[nf(m)]^{1/2}$ were all within 2% of one another and the relaxation times were well within the experimental errors shown.

As previously mentioned, it was possible to obtain the transmission envelope at higher magnetic fields when no reference signal was added. In order to compare this directly with the usual dc Shubnikov-de Haas measurements, dc Shubnikov-de Haas measurements were done on the same sample, albeit a bit crudely, by attaching current leads to two faces of the sample and two potential leads to the third face which was at right angles to the magnetic field. (The length

FIG. 4. A plot of fringe index N versus $1/B$ from the data of Fig. 3. The actual value of the fringe index is somewhat arbitrary, as the extrapolated straight line does not normally go through the origin.

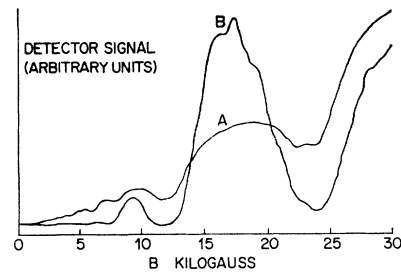
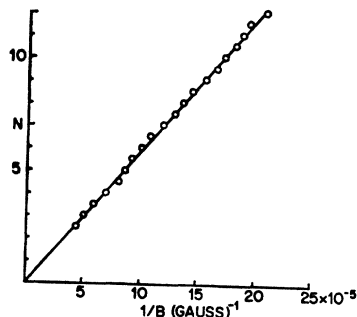


FIG. 5. The dc magnetoresistance (A) and the transmission envelope for Alfvén waves (B) versus magnetic field at 1.5°K. The magnetic field is parallel to the bisectrix axis and for A the current is parallel to the binary axis. For B the E field is parallel to the binary axis.

to cross-section ratio in this experiment was less than one, so the geometry was not ideal.) Figure 5 shows simultaneously the dc Shubnikov-de Haas effect and the transmission envelope, both with the same orientation of magnetic and electric field and temperature.

V. DISCUSSION

i. Mass Density

As there are only five equations and seven unknowns in Table I, a unique solution for all the unknowns is not possible. Instead some other procedure of analyzing the results will have to be followed.

Before this is done it should be noted that although from symmetry arguments alone, ϵ_{11}^3 and ϵ_{22}^3 should have the same value, the measured values of $[nf(m)]^{1/2}$ do not agree. The fact that the mass density in this direction is very sensitive to the direction of the magnetic field, may be the reason for the different values obtained for the two electric-field directions. A difference in alignment of around 1° could possibly account for a change of about this amount as the term m_4^2/m_3 is very sensitive to direction; m_4^2/m_3 vanishes when the magnetic field is about 6°–9° from the trigonal axis.

One method of checking the results obtained here, which is also the one followed by Williams,⁴ is to calculate n , the number of charge carriers, using the various sets of mass components in the literature. This has been done in Table II for the mass parameters of Galt *et al.*,³ Smith *et al.*,¹⁹ Kao²⁰ and SBR.¹⁸ A number of things are immediately apparent from this table. The values of n for a given set of mass parameters are reasonably consistent, deviating by at most 30% from the mean. It can also be seen that the values of n tend to group according to the direction of the magnetic field. However, the mean values of n are low compared with those reported in the literature. The best agreement is obtained when the masses of SBR are used where

¹⁹ G. E. Smith, L. C. Hebel, and S. J. Buchsbaum, *Phys. Rev.* **129**, 154 (1963).

²⁰ Yi-Han Kao, *Phys. Rev.* **129**, 1122 (1963).

TABLE II. Values of n calculated from various sets of experimental masses.

	$nf(m)$ $\times 10^{-17}$	$n(\text{calculated}) \text{ cm}^{-3} \times 10^{-17}$			
		Galt <i>et al.</i> ^a	Smith <i>et al.</i> ^b	Kao ^c	SBR ^d
ϵ_{22}^1	1.840	1.9 ^a	2.3 ¹	2.3 ^b	2.5 ⁷
ϵ_{33}^1	1.318	1.9 ¹	2.6 ⁸	2.0 ²	2.7 ⁴
ϵ_{11}^2	2.125	2.2 ⁸	2.7 ⁵	2.7 ⁶	3.0 ⁴
ϵ_{33}^2	0.213	2.2 ⁴	2.8 ⁹	2.3 ⁵	3.0 ³
ϵ_{11}^3	0.992	2.2 ⁹	1.9 ⁶	2.4 ⁷	2.1 ⁵
ϵ_{22}^3	0.924	2.1 ⁴	1.8 ⁴	2.3 ¹	2.0 ¹
Mean	n	2.1 ⁴	2.3 ⁹	2.3 ⁸	2.5 ⁹

^a Galt *et al.*, Ref. 3.^b Smith *et al.*, Ref. 19.^c Kao, Ref. 20.^d Smith, Baraff, and Rowell, Ref. 18.

the first four results agree within 10% of their reported value of $2.75 \times 10^{17}/\text{cc}$. All the results in this column can be made to agree within 10% of this value if m_4 is increased by about 25% and all other masses remain the same.

When the other mass parameters are used, still lower values of n are obtained. The most self-consistent set of values, those using the mass parameters of Galt *et al.*,³ give rise to the lowest value of all. The lowest value reported in the literature to date is that of Zitter,²¹ who gives a value of $2.5 \times 10^{17}/\text{cc}$. The trend in recent years has been away from Schoenberg's original value²² of $4.2 \times 10^{17}/\text{cc}$ towards lower values of n . The most recent values of $n(\times 10^{-17}/\text{cc})$ reported are 2.86 for the electrons by Brown,²³ 2.75 by SBR,¹⁸ 3.1 ± 0.1 by Williams,⁴ $2.89 \pm 3\%$ for the electrons and $2.99 \pm 1\%$ for the holes by Bhargava.²⁴

One possible source of error in the above results would be if the sample were not fully compensated. However, noncompensation is thought to have no effect on the results, as the starting material was the purest commercially available and was further zone refined before the sample was grown. In addition, the primary effect of noncompensation in the medium would be a rotation of the plane of polarization of the "Alfvén" wave due to a slightly different refractive index for the left and right circularly polarized waves. No effects due to a rotation of the plane of polarization could be discerned in this work.

Listed in Table III are results obtained in this paper for $[nf(m)]^{1/2}$ together with the results obtained by other workers. It was necessary to reduce the results of some of these workers to the $[nf(m)]^{1/2}$ formalism. Some of these results were obtained for Alfvén waves propagating at right angles to the magnetic field, but

²¹ R. N. Zitter, Phys. Rev. **127**, 1471 (1962).²² D. Schoenberg, Phil. Trans. Roy. Soc. (London) **A245**, 1 (1952).²³ R. D. Brown, Bull. Am. Phys. Soc. **9**, 264 (1964).²⁴ R. N. Bhargava, Bull. Am. Phys. Soc. **10**, 605 (1965); S. H. Koenig (private communication).TABLE III. Table of $[nf(m)]^{1/2}$ obtained by various workers (units $\text{cm}^{-3/2} \times 10^{-9}$). The asterisk shows which results were obtained for $\mathbf{k} \perp \mathbf{B}$. All the others were for $\mathbf{k} \parallel \mathbf{B}$.

$H \parallel$ axis	$E \parallel$ axis	Present work	Williams ^a	Faughnan ^b	Faughnan ^b	Kirsch ^c
1	2	0.429	0.481*	0.464	0.718*	0.548
1	3	0.363	0.318*	0.406	0.322*	0.378
2	1	0.461	0.470*	0.700	0.602*	
2	3	0.146	0.162*	0.140	0.171*	
3	1	0.315	0.393*	0.362	0.322*	
3	2	0.304	0.460*	0.478	0.400*	0.312*

^a Reference 4.^b Reference 12.^c Reference 7. Using $n = 3 \times 10^{17}/\text{cc}$.

the theory predicts the same values of $nf(m)$ here as when the waves propagate along the magnetic field. The agreement is poor and there appears to be no pattern to the results. As the differences are larger than the quoted errors, it is thought that the discrepancies lie in the different experimental arrangements used,²⁵ combined with the anisotropy of bismuth and an inadequate theory, especially as regards the boundaries of the media. A detailed argument as to the relative merits of the different geometries will not be gone into here but it should be noted that the spread in the values of n using the same sets of mass parameters is very much lower in the present work than in previous results.^{4,12}

All experimental masses show that ϵ_{22}^1 and ϵ_{11}^2 should differ by less than 1% with $\epsilon_{22}^1 > \epsilon_{11}^2$. Other workers^{4,12} with $\mathbf{k} \perp \mathbf{B}$ find $\epsilon_{22}^1 > \epsilon_{11}^2$ but by far more than 1%. This work finds that $\epsilon_{22}^1 < \epsilon_{11}^2$ by about 20% which makes any detailed analysis of the results using the previously discussed model of bismuth impossible. Faughnan¹² for $\mathbf{k} \parallel \mathbf{B}$ also finds that $\epsilon_{22}^1 < \epsilon_{11}^2$ but by over 30%. This seems to indicate a basic difference in the results for the two different geometries. It is obvious that the present theory cannot account for the above discrepancies. Better agreement may be obtained for these and other orientations if the nonparabolicity of the bands is taken into account.²⁶

ii. Relaxation Times

The relaxation times obtained are also listed in Table I. A number of factors, besides the mathematical complexity, do not make it worthwhile to assume a set of effective masses, a value for n and to calculate five of the mobility tensor components in terms of the sixth. These factors include the large experimental error, the inconsistency of the ϵ_{22}^1 and ϵ_{11}^2 results, and the fact that one is only measuring an average value in a given magnetic-field range (about 3 000 to 15 000 G).

However, even though the experimental errors are large, the results clearly indicate that bismuth does not have an isotropic relaxation time. One possible model is that the holes and electrons have isotropic or

²⁵ The author is indebted to G. A. Williams for a discussion on this point.²⁶ M. Cohen, Phys. Rev. **121**, 387 (1961).

nearly isotropic²¹ relaxation times which differ significantly from each other. This model would require that in the orientations, in which the holes dominate the mass density ($\epsilon_{22}^1, \epsilon_{11}^2, \epsilon_{33}^2$), the relaxation times should have consistently higher²¹ (or lower) values than in the orientations in which the electrons dominate the mass density ($\epsilon_{33}^1, \epsilon_{11}^3, \epsilon_{22}^3$). The present results do not support this model but indicate that the holes and electrons both have anisotropic relaxation times and that the average relaxation time of the holes does not differ greatly from that of the electrons.

Galt *et al.*³ use various values of $\omega\tau$ to interpret their cyclotron resonance results. However, their choice of $\omega\tau$ does not agree with the present results in so far as they associate a short relaxation time with the electrons (especially the heavy electrons) when the magnetic field is along the binary axis, while the present work finds, in the electron mass dominated ϵ_{33}^1 direction, a particularly long relaxation time.

The magnitude of the results for τ agrees very well with those measured by Zitter²¹ (0.16–0.5 nsec) and Esaki and Heer²⁷ (0.27 nsec).

iii. Shubnikov–de Haas Effect

The transmission envelopes of the Alfvén waves were measured so that the positions of the maxima and minima could be more easily ascertained. The dc Shubnikov–de Haas effect was measured partially to confirm the positions of the maxima and minima but mainly to see the relative amplitude of the oscillations obtained by the two different methods. Kawanura *et al.*¹¹ had previously remarked that the modulation due to the Shubnikov–de Haas effect is surprisingly large. These results are shown in Fig. 5 and it can be seen that the positions of the minima of the Alfvén-wave transmission agree with the resistivity minima but that the oscillations are far more marked for the transmission envelope. This is thought to be due to the following reasons: Firstly, that the transmission envelope is detected by a system with approximately square-law characteristics, and secondly, that the relaxation time appears exponentially in the imaginary part of the refractive index. The magnitude of this second effect can be seen as follows; for large $\omega\tau$, the transmission (T) is proportional to $e^{-kd/2\omega\tau}$; therefore $\Delta T/T = (kd/2\omega\tau)(\Delta\tau/\tau)$ and $kd/2\omega\tau$ is about 2 at 25 kG and 4 at 12 kG in Fig. 5. (This enhancement of the oscillations could possibly be used to advantage, especially at lower fields where the enhancement is larger, in a more detailed study of the Shubnikov–de Haas effect.) Similar curves were taken for other

orientations with similar results. As only the oscillations at high magnetic fields could be observed, the Shubnikov–de Haas periods could not be obtained. The positions of the high-field maxima and minima showed excellent qualitative and reasonable quantitative agreement with the results of SBR including spin splitting of the holes along the trigonal axis.

When one looks at the relative contribution to the mass density of the electrons and holes, one would think that in ϵ_{22}^1 and ϵ_{11}^2 the holes should dominate the Shubnikov–de Haas effect as they contribute about 98% of the mass density, but examination of the transmission curves shows that it is mainly the electrons that determine the transmission envelope. This would seem to indicate that the heavy masses are associated with long relaxation times and vice versa, which is not unreasonable. One must, however, also bear in mind that the electrons, when the magnetic field is along the binary or bisectric axis, are near or in the quantum limit, so that the relative change of τ for the electrons could be much greater than for the holes.

iv. Summary

Alfvén waves have been used to measure the mass densities and relaxation times in a single crystal of bismuth. The mass densities do not agree very well with those of previous workers. They do, however, show reasonable internal consistency when previously obtained mass parameters are used to calculate the number of carriers. The values of n are in most cases much lower than the values currently reported in the literature. When the mass parameters of SBR¹⁸ are used, the agreement with their value of n is good. The relaxation times measured are difficult to interpret as they are some weighted (by the effective masses) function of the individual relaxation times of the different groups of charge carriers. However, they do indicate that bismuth has an anisotropic relaxation time, and in magnitude agree very well with relaxation times measured using other methods. The positions of the minima in the transmission of the Alfvén waves agree with the resistivity minima as they should and the position of both agree reasonably well with those obtained by SBR.¹⁸

ACKNOWLEDGMENTS

The author would like to thank Dr. P. Erdős, Dr. R. Jaggi, Dr. B. Lüthi and Dr. E. Pytte for helpful discussions and E. Krummenacher for much appreciated technical assistance. He is also indebted to Dr. S. H. Koenig for several helpful comments regarding this manuscript.

²⁷ L. Esaki and J. Heer, *J. Appl. Phys.* 34, 234 (1963).